Exp Biomed Res 2024; 7(1): 27-38 https://doi.org/10.30714/j-ebr.2024.205

Experimental Biomedical Research *Original article*

A novel approach for breast ultrasound classification using two-dimensional empirical mode decomposition and multiple features

Şerife Gengec Benli*[1], Zeynep Ak[2]

[1]*Biomedical Engineering, Engineering Faculty, Erciyes University, Kayseri, Türkiye*

[2]*Biomedical Engineering Dept., Graduate School of Natural and Applied Sciences, Erciyes University, Kayseri, Türkiye*

ABSTRACT

Aim: Breast cancer stands as a prominent cause of female mortality on a global scale, underscoring the critical need for precise and efficient diagnostic techniques. This research significantly enriches the body of knowledge pertaining to breast cancer classification, especially when employing breast ultrasound images, by introducing a novel method rooted in the two dimensional empirical mode decomposition (biEMD) method. In this study, an evaluation of the classification performance is proposed based on various texture features of breast ultrasound images and their corresponding biEMD subbands.

Methods: A total of 437 benign and 210 malignant breast ultrasound images were analyzed, preprocessed, and decomposed into three biEMD sub-bands. A variety of features, including the Gray Level Co-occurrence Matrix (GLCM), Local Binary Patterns (LBP), and Histogram of Oriented Gradient (HOG), were extracted, and a feature selection process was performed using the least absolute shrinkage and selection operator method. The study employed GLCM, LBP and HOG, and machine learning techniques, including artificial neural networks (ANN), k-nearest neighbors (kNN), the ensemble method, and statistical discriminant analysis, to classify benign and malignant cases. The classification performance, measured through Area Under the Curve (AUC), accuracy, and F1 score, was evaluated using a 10-fold cross-validation approach.

Results: The study showed that using the ANN method and hybrid features (GLCM+LBP+HOG) from BUS images' biEMD sub-bands led to excellent performance, with an AUC of 0.9945, an accuracy of 0.9644, and an F1 score of 0.9668. This has revealed the effectiveness of the biEMD method for classifying breast tumor types from ultrasound images.

Conclusion: The obtained results have revealed the effectiveness of the biEMD method for classifying breast tumor types from ultrasound images, demonstrating high-performance classification using the proposed approach.

Keywords: Breast ultrasound images, two dimensional empirical mode decomposition, subbands, classifications.

✉ *Şerife Gengec Benli**

Biomedical Engineering, Engineering Faculty, Erciyes University, Kayseri, Türkiye

E-mail: serifegengec@gmail.com

Received: 2023-11-02 / Revisions: 2023-12-02

Accepted: 2023-12-07 / Published: 2024-01-01

Introduction

Breast cancer is a significant healthcare challenge and a leading cause of cancer-related global mortality among women [1]. Early

detection and treatment contribute to achieving enhanced survival rates and obtaining better clinical outcomes among patients diagnosed with breast cancer. Among the most effective techniques for detecting breast cancer are medical imaging modalities such as magnetic resonance imaging, mammography, and ultrasound. Ultrasound is often considered a primary method for imaging breast lesions since it is widely available, cost-effective, has good diagnostic accuracy, and may provide noninvasive imaging capabilities [2,3,4]. Furthermore, it is sensitive to speckle noise, which can make working with ultrasound images challenging [5]. So, this characteristic requires a robust preprocessing procedure. Studies based on the classification of breast ultrasound (BUS) images, which are improved through preprocessing and contain features obtained from images that are challenging for radiologists to analyze, have gained momentum with the increasing use of artificial intelligence applications [6].

In a study conducted by Gomez et al., a technique based on watershed transformation was used to segment 413 benign and 228 malignant BUS images. They calculated 22 morphological features from the segmented images. The obtained features were classified using Fisher linear discriminant analysis, and the area under the curve (AUC) value was found to be 0.953 [7]. In another study, Cai et al., proposed a phase and texture-based approach to classify 69 benign and 69 malignant breast lesion ultrasound images. In the classification using support vector machine (SVM), an accuracy of 0.8696 was achieved [8]. In the study proposed by Huang et al., filtering was performed to eliminate noise, and the lesion area was extracted using red, green, and blue (RGB) segmentation. Features were extracted from the segmented lesion regions using gray-level histograms, gray-level co-occurrence matrices (GLCM), and original gradient histograms (HOG) methods, and they were classified with SVM classifier with an accuracy of 0.95 [9]. Moon et al. conducted a classification study with an accuracy of 0.9481 using SVM based on tissue features of segmented lesions from 169 ultrasound images [10]. In a study involving 70 benign and 50 malignant BUS images, after segmentation, a total of 40 features were extracted both morphologically and texturally. The study, which achieved an accuracy of 0.9585 using an SVM classifier, was proposed by Prabusankarlal et al [11]. A total of 283 BUS images, comprising benign and malignant lesions, were used to extract various features using the BI-RADS method. The extracted features were classified using decision trees, SVM, random forest, and k-Nearest Neighbor (kNN) classifiers. The highest AUC value was found to be 0.84 with SVM, while the highest accuracy was 0.78 with RF. This study, which evaluates the performance of various classifiers, was proposed by Shan et al. [12]. In a study conducted by Byra, features of benign and malignant breast lesions were extracted using the VGG19 transfer learning method and classified using Fisher Discriminant Analysis. The study concluded with an AUC value of 0.826 and an accuracy of 0.77 [13]. In another study by Byra et al., transfer learning methods were used with 678 benign and 204 malignant lesion-containing BUS images. The model that separates ultrasound images into RGB layers, and extracts features from Max Pooling (MP) and Fully Connected (FC) layers, was applied to an SVM classifier as input. In the study repeated with the UDIAT and OASBUD datasets to evaluate the performance of the same model, an accuracy of 0.83 was achieved with the SVM classifier [14]. In a study proposed by Priya et al., the Breast Ultrasound Images (BUSI) dataset was used, and images segmented with the

K-means method were classified using three different machine learning methods. They achieved a classification process with an accuracy of 0.9587 using Logistic Regression (LR), 0.9714 using Random RF, and 0.9333 using kNN [15].

In recent years, deep learning models have become widely preferred for breast cancer detection. In a study proposed by Han et al., a total of 7408 BUS images, consisting of 4254 benign and 3154 malignant lesions, were classified with an accuracy of 0.9 using the GoogleNet architecture [16]. Another deep learning study was proposed by Raza et al., and colleagues. In this study, conducted using the DeepBreastCancerNet deep learning model, an accuracy of 0.9935 was achieved for breast cancer classification [17] .

Reviewing the existing literature reveals that breast cancer classification is being carried out using various datasets and applying machine learning and deep learning techniques. The purpose of this research is to provide a novel method based on image processing to the existing literature for the classification of BUS images, including benign and malignant lesions. Using the BUSI dataset and the recommended methodology, this research performed classification to differentiate between different forms of breast cancer. In addition, it is novel since it is the first technique of its kind to classify BUS images based on characteristics extracted from biEMD sub-bands. Taking into account the influence of the tissue surrounding the tumor is also included in this study. This research provides for a more nuanced analysis of BUS images by highlighting the unique characteristics that may be seen in each sub-band. It has been discovered in this study that the biEMD sub-bands may be used to classify lesions with more precision than before without resorting to time-consuming manual segmentation techniques.

Materials and methods

This section describes the dataset, preprocessing, feature extraction, data balancing, feature selection, and classification algorithms utilized in the proposed approach.

Dataset: The data utilized for the analysis of breast lesions in this research were acquired from the BUSI dataset, which was made publicly available and was compiled by Dhabyani et al [18]. The dataset consists of 780 images of different sizes with an average resolution of 500x500 pixels. The images are classified into the following three categories: benign (487 images), malignant (210 images), and normal (133 images) (Figure 1). The sample for this study comprised 600 female patients, whose ages

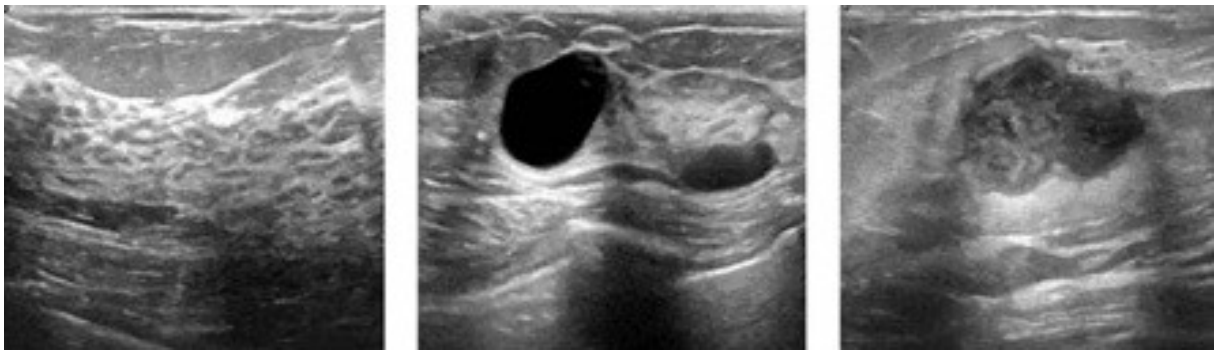

Normal Benign Malignant

Figure 1. Examples of ultrasound breast images dataset.

varied from 25 to 75 years. In the proposed research, raw BUS images of 437 benign and 210 malignant breast tumors were utilized to differentiate between these two groups.

The data presented in the article contributes to studies on the classification, detection and segmentation of breast cancer by enabling the analysis of breast ultrasound images with machine learning methods. In this study, the biEMD method, which offers an innovative approach to the classification of breast cancer, was comprehensively examined using the BUSI dataset.

Preprocessing of breast ultrasound images: The low contrast of ultrasound images makes them vulnerable to segmentation and classification techniques. Thus, the BUS images have so undergone a number of preprocessing procedures. Since the dataset in which the study was carried out contained images of different sizes, all images were resized to 256 * 256 in order to have the same sensitivity of the extracted features. The median filter, which is often used for noise reduction in ultrasound images, was first used. In this study, the median filter was selected because of its effective noise reduction and its sensitivity to edges. A notable feature extraction takes place in the transition zone between tumor and healthy tissue by this technique [19]. To further distinguish tumor tissue from normal tissue, gray level contrast enhancement [20] was applied to the ultrasonic images with low contrast.

Subband decomposition method: In this study, features were extracted from preprocessed raw (p-raw) BUS images and their two dimensional empirical mode decomposition (biEMD) images. biEMD method was used as sub-band decomposition approach described below.

Two-dimensional empirical mode decomposition: Empirical Mode Decomposition (EMD), an approach applied to signals, facilitates the analysis of complex signals by separating them into amplitude and frequency forms [21]. The primary method considered in this study is two-dimensional Empirical Mode Decomposition (biEMD), which is a distinct version of EMD developed for the purpose of applying it to two-dimensional data or images. biEMD extracts features at multiple scales or spatial frequencies and contributes to various image processing methods. Nunes et al., have developed the biEMD method to operate at multiple scales and spatial frequencies to extract texture and filter noise. They tested the performance of the method by extracting different numbers of intrinsic mode functions (IMF) from different image types [22]. It is commonly used in tasks such as texture extraction and noise filtering. Nunes et al., and colleagues In another article, he explained the formula they developed for biMED with Equation 2.1 [23]. The method is detailed with mathematical formulas and derivations in the referenced study [22]. After preprocessing, BUS images were decomposed to biEMD, resulting in their decomposition into different sub-bands. When examining the sub-bands for all the data in the dataset, the images were decomposed into three sub-bands and one residue. The features that form the foundation of classification were extracted using these sub-bands.

$$Irec_I = V_{n\geq 1}\partial_1^n(J) \qquad \text{Equation (2.1)}$$

$\mathrm{Irec_I}$, refers to the grayscale reconstruction of I from J. Irec stands for reconstructed image I original image.

Feature Extraction

The purpose of feature extraction is to identify and interpret significant attributes of raw data in a reduced-dimensional space. For this study, we used three techniques such as gray level co-occurrence matrix, local binary pattern, histogram of oriented gradient to extract textural

features from preprocessed raw images and biEMD subbands image. The following sections provide a detailed explanation of each methodology.

Gray Level Co-occurrence Matrix: Gray Level Co-occurrence Matrix (GLCM), a technique introduced by M. Haralick, serves as a feature extraction method that characterizes the association between adjacent pixels within a grayscale image [24]. The initial pixel is referred to as the "reference pixel," while the other is known as the "neighboring pixel." The distribution within the matrix is modified based on the pixel distance and the angle between them. This matrix takes the form of a square matrix with a size of N and forecasts a function that describes the collective probability distribution of gray level pairs in an image [25]. In this study, second-order statistical features such as autocorrelation, cluster prominence, cluster shade, contrast, correlation1, correlation2, difference entropy, difference variance, dissimilarity, energy, entropy, homogenity1, homogenity2, maximum probability, sum average, sum entropy, sum of squares, sum variance, information measure of correlation1, information measure of correlation2, inverse difference, inverse difference normalized, inverse different moment, kurtosis, skewness, maximal correlation coefficient, and mean were calculated for BUS images via GLCM. A total of 27 texture properties were computed from BUS images via GLCM, which provide a quantitative description.

Local Binary Patterns: The Local Binary Pattern (LBP) technique is used to characterize the texture of an image by comparing the intensity values of each pixel with those of its nearby pixels [26]. Subsequently, the result of this comparison is transformed into a binary code. The dimension of the LBP descriptor is determined by the quantity of sample points (P) and the radius (R) of the circular neighborhood around the center pixel. The total number of distinct patterns for a given number of sample points, P, may be calculated using the following method:

$$U(P) = P * (P - 1) + 3$$

The feature size corresponds to U(P), which represents the length of the LBP histogram. In this suggested research, the feature size will be $U(8) = 8 * (8 - 1) + 3 = 59$ when utilizing the most typical LBP setup with P = 8 sample points and R = 1, as described in the default option. The LBP histogram consists of 59 values, serving as a feature vector for further analysis, such as image classification or similarity assessment. The selected LBP parameters (P and R) may influence the feature size, therefore alternative configurations may be better appropriate for certain applications or datasets.

Histogram of Oriented Gradient: Histogram of Oriented Gradient (HOG) is a robust descriptor which is widely used machine vision and image processing for object detection and image classification processes. HOG is built upon the premise that the local appearance and shape of an object in an image can be effectively described by the distribution of local intensity gradients or edge directions, which are inherently perpendicular to the gradient's direction. HOG generates a feature vector that encapsulates the visual characteristics of objects by analyzing the local gradients within an image. The key steps for computing HOG features can be outlined as follows: gradient computation, orientation binning, feature description, and L2 normalization [27].

In this study, following the resizing process, a manual cell size of 'CellSize' was set to [64 64] for each image, and a total of 324 features were extracted by creating an HOG architecture. Automatic extraction of HOG features could significantly increase the data size, potentially

adversely affecting classification performance. Therefore, manual feature extraction with a specific cell size was employed.

Data balancing

There are various methods to better represent the minority class and reduce the class imbalance problem in biomedical data. Resolving the class imbalance is often accomplished by data augmentation and downsampling. The Adaptive Synthetic sampling technique (ADASYN) was used in the proposed research to produce synthetic minority samples via data augmentation. This resulted in a balanced distribution of samples throughout the several categories into which the dataset was divided [28]. Throughout this study, data balance between classes was maintained in all classifications using the ADASYN method.

Feature selection

The current study used the Least Absolute Shrinkage and Selection Operator (LASSO) approach for the purpose of feature selection. The LASSO, a statistical technique pioneered by Tibshirani [29], is used in regression analysis for parameter estimation and variable selection. This technique has the capacity to provide an analytical solution and a low-variance estimate that can be easily comprehended in the context of linear regression.

Classification

Following the extraction and selection of features using the techniques described above, different machine learning algorithms such as artificially intelligent networks, k-nearest neighbors algorithm, ensemble classifier and discriminant analysis were used and compared in terms of their performance in identifying BUS images as malign and benign. A short summary of the algorithms performed is provided below.

Artificial Neural Network (ANN) is a machine learning algorithm modeled based on the working principles of the nerve cells in the human brain and is employed to learn complex relationships in large datasets. ANN, successfully used in classification, prediction, and pattern recognition tasks, features a structure organized into layers with numerous neurons or nodes. Generally, ANN can be divided into three layers of neurons: the input layer, which receives data; the hidden layer, responsible for pattern extraction and most of the internal processing; and the output layer, which generates and provides the ultimate network results [30,31].

KNN calculates similarity measures of data by using the k nearest data points in its vicinity to determine the class or value of a data point, facilitating the grouping of data points. The value of k determines the number of neighbors in kNN, and the larger the k value, the more neighbors are utilized, resulting in smoother predictions, but overfitting can occur. Conversely, the smaller the k value, the more accurate the predictions become, but it becomes more susceptible to noise. Therefore, the k value is typically optimized through trial and error or cross-validation [32].

Ensemble method is based on the idea of creating a stronger learner by bringing together multiple weak learners (e.g., decision trees, logistic regression, etc.) or networks. Ensemble methods are commonly used to achieve more accurate and generalizable results by combining the predictions of multiple learners instead of a single learner. The advantages of ensemble methods include higher prediction accuracy, the ability to improve generalization, reducing overfitting, and achieving more balanced outcomes [33].

Statistical discriminant analysis is used to classify data points into two or more classes. This method measures the differences between classes and within-class similarities to identify the best discriminating features. In this way, it is used to

predict to which class new data points belong [34].

In this study, values for every classifier parameter were determined utilizing the Bayesian optimization method. Normalization was performed on the feature vector that was supplied as input to the classifier, resulting in a mean of zero and a standard deviation of one. Figure 2 illustrates the framework of the study.

these approaches, essential features for classification have been identified through the LASSO method. The effectiveness of biEMD subbands and p-raw images in distinguishing between benign and malignant BUS images has been assessed through various techniques, including ANN, kNN, ensemble methods, and discriminant analysis. Performance metrics for binary classification, such as the AUC, accuracy,

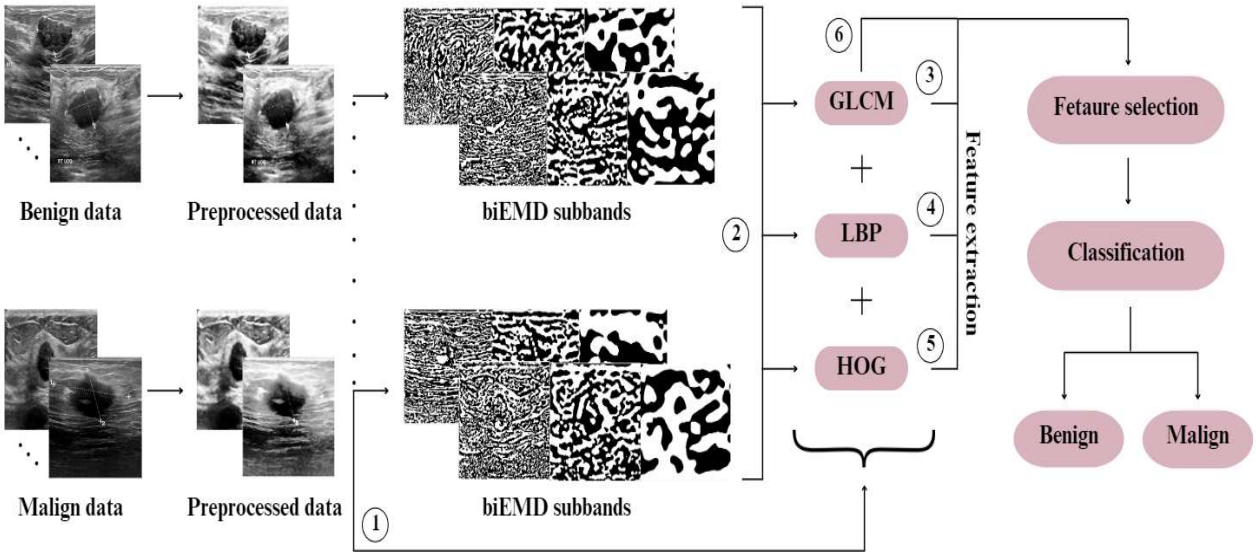

Figure 2. Representation of the classification process of preprocessed raw images and biEMD subbands images.

Results and Discussion

BUS scans of 437 benign cases and 210 malignant cases were analysed in the proposed study. The quality of ultrasonic images has been improved by first applying a median filter and contrast enhancement. Subsequently, the preprocessed BUS images were processed using the biEMD sub-band decomposition method, resulting in three sub-bands. During the feature extraction step, various features such as GLCM, LBP, and HOG, were obtained from preprocessed raw images and their corresponding 3 biEMD sub-bands. Furthermore, within both of

and F1 score, have been used to evaluate the classification results. The AUC value is a metric that defines the true positive rate as a function of the false positive rate, expressed as the area under the ROC curve. Accuracy is a metric frequently used to measure the performance of classifiers, it relates the true value and predicted values in the confusion matrix. F1 score is a metric that provides more precise information, obtained by the weighted average of precision and recall functions. Equations related to Accuracy and F1 metrics are given in Equations 3.2 and 3.3, respectively [35]. Tables 1 and 2 display the average classification performance for all images

using p-raw images and biEMD subband images, respectively. An analysis of these tables provides insight into the classification performance achieved when utilizing features extracted from both p-raw images and biEMD subband images.

$$Acc = \frac{TP+TN}{TP+FP+TN+FN} \quad \text{Equation (3.2)}$$

TP is expressed as true positive, FP as false positive, TN as true negative, FN as false negative.

$$F_1 = 2.\frac{P.R}{P+R} \quad \text{Equation (3.3)}$$

P is the precision function, R is the recall function.

During the classification study, the training and testing datasets were determined through a 10-fold cross-validation methodology. Each classification procedure underwent ten iterations, and the tables presented display the average performance results from these iterations.

The study presented the results of classification performance based on 10 trials employing 10-fold cross-validation through box plots. Visual analysis highlights the strength of the proposed classification models and the consistency of the results, as depicted in Figure 3. Box plots effectively illustrate the central tendency, variation, and potential anomalies in the outcomes obtained from several trials.

Table 1. Binary classification results in various types of textural features obtained from preprocessed raw BUS images**.**

Type of texture features	**ANN**			**kNN**			**Ensemble**			**Discriminant**		
	AUC	**Acc**	**F1**	**AUC**	**Acc**	**F1**	**AUC**	**Acc**	**F1**	**AUC**	**Acc**	**F1**
GLCM	0.7694	0.7234	0.7196	0.7337	0.7322	0.7393	0.7722	0.7120	0.7061	0.6444	0.6080	0.5790
LBP	0.9123	0.8507	0.8554	0.8386	0.8348	0.8488	0.9340	0.8684	0.8684	0.7708	0.6969	0.6862
HOG	0.9565	0.9013	0.9001	0.8959	0.8920	0.8954	0.9554	0.8927	0.8892	0.8712	0.7969	0.7895
Hybrid	0.9722	0.9177	0.9233	0.9018	0.9038	0.9126	0.9684	0.9204	0.9245	0.9159	0.8336	0.8416

**Hybrid: GLCM+LBP+HOG*

Table 2. Binary classification results in various types of textural features obtained from the biEMD subband of preprocessed raw BUS images.

Type of texture features	**ANN**			**kNN**			**Ensemble**			**Discriminant**		
	AUC	Acc	F1	AUC	Acc	F1	AUC	Acc	F1	AUC	Acc	F1
GLCM	0.8808	0.8273	0.8409	0.8277	0.8285	0.8493	0.9179	0.8444	0.8515	0.7358	0.6729	0.6765
LBP	0.9304	0.8654	0.8713	0.8394	0.8366	0.8534	0.9345	0.8689	0.8692	0.8359	0.7567	0.7544
HOG	0.9881	0.9491	0.9523	0.8957	0.8990	0.9102	0.9862	0.9434	0.9463	0.9854	0.9383	0.9417
Hybrid	0.9945	0.9644	0.9668	0.9196	0.9228	0.9307	0.9874	0.9506	0.9533	0.9939	0.9608	0.9632

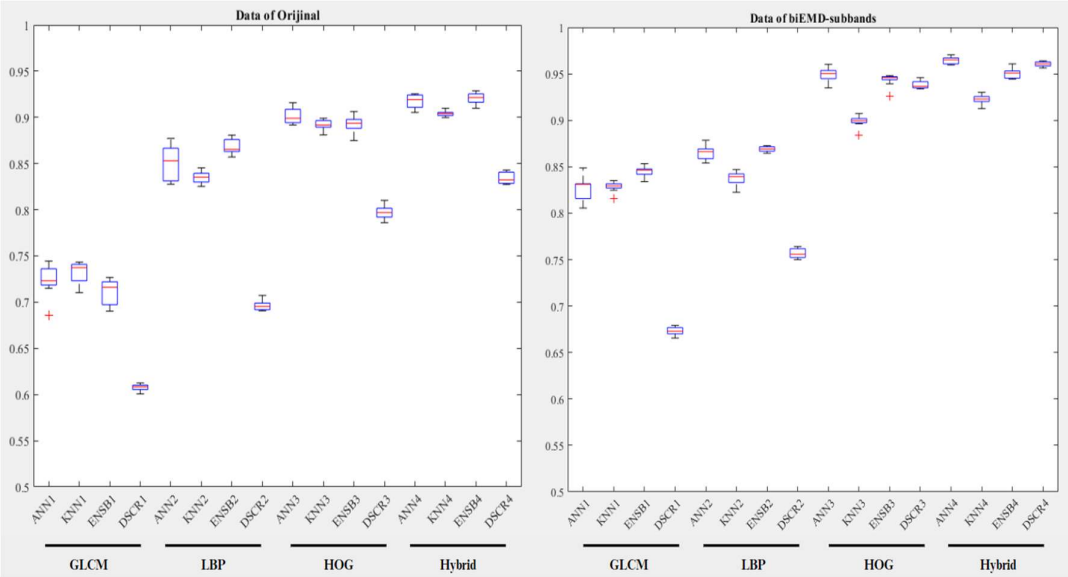

Figure 3. Box plots of classification accuracy obtained various textural features.

Conclusions

In this study, 437 benign and 210 malign BUS images were analyzed thoroughly utilizing a 2D empirical mode decomposition technique. Feature extraction was performed on both the p-raw images and the 3 biEMD sub-bands. Data balancing was achieved using the ADASYN method to ensure that classification models perform more evenly and exhibit better performance. Using the LASSO method, the most significant features were determined for classification in both approaches.

In this proposed study, a new approach was employed by decomposing BUS images into biEMD sub-band images to obtain their different domain-specific features. This approach allowed for the extraction of important features from BUSI images for the detection of BUS images from multiple perspectives. Using machine learning techniques such as ANN, kNN, ensemble methods, and discriminant analysis, the study presented a new method in the literature based on the feature and classifier combination that achieved the best classification performance. As shown in Table 2, the classification results based on GLCM features calculated from biEMD subbands using the ensemble method averaged 84.44% over 10 trials, while LBP features and the ensemble method yielded 86.89%, HOG features and ANN achieved 94.91%, and all features with ANN resulted in a 96.44% classification success rate. As indicated in Table 1, in the approach that employed preprocessed raw BUs images without decomposing them into sub-bands and utilized GLCM, LBP, HOG, and hybrid features with machine learning methods, a lower classification performance was obtained compared to the biEMD-feature-machine learning approach. Based on these results, a high-performance classification model for BUS image detection was proposed, utilizing biEMD sub-band images and hybrid features consisting of GLCM, LBP, and HOG features, along with an ANN model.

When our study is compared with the studies in the literature, it is seen that the results obtained are more productive than most of the existing studies. When a general comparison is made, machine learning methods and Gomez et al.

0.953 accuracy [7], Moon et al. 0.9481 accuracy [10], Shan et al. 0.78 accuracy [12], Byra et al. 0.83 accuracy [14], and Priya et al. It achieved an accuracy of 0.9714 [15]. In addition, an accuracy of 0.9935 was achieved with DeepBreastCancerNet, one of the deep learning approaches that has been widely used for breast cancer segmentation and classification in recent years. The highest accuracy of 0.9644 was achieved with the proposed method, and the presented study will make a significant contribution to the literature as it is an innovative method and achieves high accuracy. For higher performance in deep learning studies, a high-dimensional data set is required and this is a costly and long process. It is seen that high accuracy is achieved with the presented approach without using high-dimensional data.

The low resolution and speckle noise of the ultrasound images used in the study may negatively affect the quality of the extracted features and classifier performance. Even if the necessary preprocessing is performed for this issue, it may not be possible to completely eliminate noise and distinguish tumor tissue from normal tissue. In addition, working with two-dimensional data and its subbands is a disadvantageous process in terms of time and cost in terms of feature extraction. The point reached in the study is that despite all these limitations, the biEMD method achieves a remarcable performance in classifying ultrasound images.

In future studies, proposed method can be applied to the diagnosis of various types of cancer problems, aiming to establish a biEMD-feature extraction-machine learning model for the high-performance classification of various patological disorders.

Funding: *The authors received no financial support for the research, authorship, and/or publication of this article.*

Conflict of interest: *The authors declare that they have no conflict of interest.*

Ethical statement: *Not applicable.*

Data availability statement: *The performed breast ultrasound dataset, generated by Al-Dhabyani et al., can be downloaded from https://doi.org/10.1016/j.dib.2019.104863 (accessed on 10 October 2021).*

References

[1]Sung H, Ferlay J, Siegel RL, et al. Global Cancer Statistics 2020: GLOBOCAN Estimates of Incidence and Mortality Worldwide for 36 Cancers in 185 Countries. CA Cancer J Clin. 2021;71(3):209-249.

[2]Hooley RJ, Scoutt LM, Philpotts LE. Breast ultrasonography: state of the art. Radiology. 2013;268(3):642-659.

[3]Boca Bene I, Ciurea AI, Ciortea CA, Dudea SM. Pros and Cons for Automated Breast Ultrasound (ABUS): A Narrative Review. J Pers Med. 2021;11(8):703.

[4]Elawady M, Sadek I, Shabayek AER, et al. Automatic nonlinear filtering and

segmentation for breast ultrasound images. In Image Analysis and Recognition: 13th International Conference. ICIAR 2016 in Memory of Mohamed Kamel. 2016;13:206-213.

[5] Ayana G, Dese K, Raj H, et al De-Speckling Breast Cancer Ultrasound Images Using a Rotationally Invariant Block Matching Based Non-Local Means (RIBM-NLM) Method. Diagnostics (Basel). 2022;12(4):862.

[6] Dan Q, Zheng T, Liu L, et al. Ultrasound for Breast Cancer Screening in Resource-Limited Settings: Current Practice and Future Directions. Cancers (Basel). 2023;15(7):2112.

[7] Gómez-Flores W, Rodriguez A, Pereira W, et al. Feature selection and classifier performance in computer-aided diagnosis for breast ultrasound. in 2013 10th Int. Conf. Expo Emerg. Technol. a Smarter World, CEWIT 2013. 2013;1–5.

[8] Cai L, Wang X, Wang Y, et al. Robust phase-based texture descriptor for classification of breast ultrasound images. Biomed Eng Online. 2015;14:26.

[9] Huang Q, Yang F, Liu L, et al. Automatic segmentation of breast lesions for interaction in ultrasonic computer-aided diagnosis. Inf. Sci. (Ny). 2015;314:293–310.

[10] Moon WK, Huang YS, Lo CM, et al. Computer-aided diagnosis for distinguishing between triple-negative breast cancer and fibroadenomas based on ultrasound texture features. Med Phys. 2015;42(6):3024-35.

[11] Prabusankarlal KM, Thirumoorthy P, Manavalan R. Assessment of combined textural and morphological features for diagnosis of breast masses in ultrasound. Human-Centric Comput. Inf. Sci. 2015;5(1):12.

[12] Shan J, Alam SK, Garra B, et al. Computer-Aided Diagnosis for Breast Ultrasound Using Computerized BI-RADS Features and Machine Learning Methods. Ultrasound Med. Biol. 2016;42(4):980–8.

[13] Byra M. Discriminant analysis of neural style representations for breast lesion classification in ultrasound. Biocybern. Biomed. Eng. 2018;38(3):684–90.

[14] Byra M, Galperin M, Ojeda-Fournier H, et al. Breast mass classification in sonography with transfer learning using a deep convolutional neural network and color conversion. Med. Phys. 2019;46(2):746–55.

[15] Priya K, Senthilkumar V, Samson Isaac J, et al. Breast Cancer Segmentation by K-Means and Classification by Machine Learning. in: 2022 Int. Conf. Autom. Comput. Renew. Syst. 2022;651–56.

[16] Han S, Kang HK, Jeong JY, et al. A deep learning framework for supporting the classification of breast lesions in ultrasound images. Phys. Med. Biol. 2017;62(19):7714–28.

[17] Raza A, Ullah N, Khan JA, et al. DeepBreastCancerNet: A Novel Deep Learning Model for Breast Cancer Detection Using Ultrasound Images. Appl. Sci. 2023;13.

[18] Al-Dhabyani W, Gomaa M, Khaled H, et al. Dataset of breast ultrasound images, Data Brief. 2019;21;28:104863.

[19] Kumar Pal S, Bhardwaj A, Shukla AP. A Review on Despeckling Filters in Ultrasound Images for Speckle Noise Reduction. in: 2021 Int. Conf. Adv. Comput. Innov. Technol. Eng. 2021;973–78.

[20] Kapetas P, Clauser P, Woitek R, et al. Quantitative Multiparametric Breast Ultrasound: Application of Contrast-Enhanced Ultrasound and Elastography Leads to an Improved Differentiation of Benign and Malignant Lesions. Invest. Radiol. 2019;54(5):257–64.

[21] Huang NE, Shen Z, Long SR, et al. The

empirical mode decomposition and the Hilbert spectrum for nonlinear and non-stationary time series analysis. Proc. R. Soc. London. Ser. A Math. Phys. Eng. Sci. 1998;454(1971):903–95.

[22] Nunes JC, Bouaoune Y, Delechelle E, et al. Image analysis by bidimensional empirical mode decomposition. Image Vis. Comput. 2003; 21(12):1019–26.

[23] Nunes JC, Guyot S, Deléchelle E. Texture analysis based on local analysis of the bidimensional empirical mode decomposition. Machine Vision and applications. 2005;16(3):177-88.

[24] Haralick RM, Shanmugam K, Dinstein I. Textural Features for Image Classification. IEEE Trans. Syst. Man. Cybern. SMC. 1973;3(6):610–21.

[25] Baraldi A, Panniggiani F. An investigation of the textural characteristics associated with gray level cooccurrence matrix statistical parameters. IEEE Trans. Geosci. Remote Sens. 1995; 33(2):293–304.

[26] Ojala T, Pietikainen M, Maenpaa T. Multiresolution gray-scale and rotation invariant texture classification with local binary patterns. IEEE Trans. Pattern Anal. Mach. Intell. 2002; 24(7):971–87.

[27] Déniz O, Bueno G, Salido J, et al Face recognition using Histograms of Oriented Gradients, Pattern Recognit. Lett. 2011;32(12):1598–603.

[28] He H, Bai Y, Garcia EA, et al. ADASYN: Adaptive synthetic sampling approach for imbalanced learning. in: 2008 IEEE Int. Jt. Conf. Neural Networks (IEEE World Congr. Comput. Intell. 2008;1322–8.

[29] Tibshirani R. Regression Shrinkage and Selection via the Lasso. J. R. Stat. Soc. Ser. B. 1996; 58(1):267–88.

[30] Zhang G, Hu MY, Eddy Patuwo B, et al. Artificial neural networks in bankruptcy prediction: General framework and cross-validation analysis. Eur. J. Oper. Res. 1999;116(1):16–32.

[31] Hopfield JJ. Artificial neural networks. IEEE Circuits Devices Mag. 1988;4(5):3–10.

[32] Laaksonen J, Oja E. Classification with learning k-nearest neighbors. in: Proc. Int. Conf. Neural Networks, 1996;1480–3 vol.3.

[33] Chawla N, Ca N, Hall L, et al. Learning ensembles from bites: A scalable and accurate approach. J. Mach. Learn. Res. 5. 2004;5:421–51.

[34] Zhao W, Chellappa R, Nandhakumar N. Empirical performance analysis of linear discriminant classifiers. in: Proceedings. 1998 IEEE Comput. Soc. Conf. Comput. Vis. Pattern Recognit. (Cat. No.98CB36231). 1998;164–9.

[35] Jeni LA, Cohn JF, De La Torre F. Facing Imbalanced Data Recommendations for the Use of Performance Metrics. Int Conf Affect Comput Intell Interact Workshops. 2013;245-51.